AD-A076 344 NEW JERSEY INST OF TECH NEWARK F/G 20/3
RAY OPTICAL DESCRIPTION OF WAVES GUIDED BY INTEGRATED DIELECTRI--ETC(U)
OCT 79 G M WHITMAN , P LISMAN , S J MAURER DAAG29-77-G-0094
UNCLASSIFIED ARO-13677.1-ELX NL

1 OF 1
ADA 076344

END
DATE FILMED
12-79
DDC

Unclassified

SECURITY CLASSIFICATION OF THIS PAGE (When Data Entered)

(18) ARO 13677.1-ELX

REPORT DOCUMENTATION PAGE

READ INSTRUCTIONS BEFORE COMPLETING FORM

(12)

1. REPORT NUMBER (19) 13677.1-ELX

2. GOVT ACCESSION NO.

3. RECIPIENT'S CATALOG NUMBER (9)

4. TITLE (and Subtitle)

(6) Ray Optical Description of Waves Guided by Integrated Dielectric Cylinder-Cone Structures.

5. TYPE OF REPORT & PERIOD COVERED

Final Technical Report
29 Jan 1976 - 31 May 1979

6. PERFORMING ORG. REPORT NUMBER

7. AUTHOR(s)

(10) G. M. Whitman, P. Lisman, S. J. Maurer

8. CONTRACT OR GRANT NUMBER(s)

DAAG29-76-G-0131
(15) DAAG29-77-G-0094

9. PERFORMING ORGANIZATION NAME AND ADDRESS

New Jersey Institute of Technolgoy
Newark College of Engineering
Newark, New Jersey 07102

10. PROGRAM ELEMENT, PROJECT, TASK AREA & WORK UNIT NUMBERS

LPN-DRXR-EL-13677

11. CONTROLLING OFFICE NAME AND ADDRESS

U. S. Army Research Office
P. O. Box 12211
Research Triangle Park, NC 27709

(11)

12. REPORT DATE

October 1979

13. NUMBER OF PAGES

51 (12) 57

14. MONITORING AGENCY NAME & ADDRESS (if different from Controlling Office)

Department of the Army
U.S. Army Research Office
Research Triangle Park, N.C. 2770

15. SECURITY CLASS. (of this report)

Unclassified

15a. DECLASSIFICATION/DOWNGRADING SCHEDULE

16. DISTRIBUTION STATEMENT (of this Report)

Approved for public release; distribution unlimited.

17. DISTRIBUTION STATEMENT (of the abstract entered in Block 20, if different from Report)

18. SUPPLEMENTARY NOTES

The view, opinions, and/or findings contained in this report are those of the author(s) and should not be construed as an official Department of the Army position, policy, or decision, unless so designated by other documentation.

19. KEY WORDS (Continue on reverse side if necessary and identify by block number)

Tapered dielectric
Dielectric cone
Dielectric cylinder
Integrated dielectric structure
Ray optics
Asymptotic boundary conditions
Caustics

20. ABSTRACT (Continue on reverse side if necessary and identify by block number)

The techniques of ray-optics, which have provided meaningful results in the study of electromagnetic and acoustic problems, are applied to the integrated dielectric cylinder-cone configuration.

The method of geometrical optics is presented. The eiconal and transport equations are derived. Asymptotic boundary conditions are discussed and a generalized reflection coefficient introduced. Before investigating the cylinder-cone non-separable geometry, an understanding of the ray structure in both an →

DD FORM 1 JAN 73 1473 EDITION OF 1 NOV 65 IS OBSOLETE

Unclassified

SECURITY CLASSIFICATION OF THIS PAGE (When Data Entered)

392 024 (19) 11 07 79

infinite dielectric cylinder and, separately, in an infinite dielectric cone is needed. This is accomplished in the report and, consequently, amplitude and phase information is attained. In addition, caustics are discussed. Caustics are envelopes of the ray systems and, thus, are surfaces which separate propagating and non-propagating (or complex evanescent) regions and characterize the modal ray systems in non-uniform regions. The report concludes with a discussion of the transition region between the cylinder and the cone.

RAY-OPTICAL DESCRIPTION OF WAVES GUIDED BY INTEGRATED DIELECTRIC CYLINDER-CONE STRUCTURES

by

G. M. Whitman, New Jersey Institute of Technology, N.J.

P. Lisman, The Analytic Sciences Corp., Mass.

S. J. Maurer, New York Institute of Technology, N.Y.

October 1979

Prepared for

U.S. Army Research Office

Research Triangle Park, N.C. 27709

Contract No. DAAG29-77-G-0094

Project No. DRXRO-EL-13677

New Jersey Institute of Technology

Newark, New Jersey 07102

ABSTRACT

The techniques of ray-optics, which have provided meaningful results in the study of electromagnetic and acoustic problems, are applied to the integrated dielectric cylinder-cone configuration.

The method of geometrical optics is presented. The eiconal and transport equations are derived. Asymptotic boundary conditions are discussed and a generalized reflection coefficient introduced. Before investigating the cylinder-cone non-separable geometry, an understanding of the ray structure in both an infinite dielectric cylinder and, separately, in an infinite dielectric cone is needed. This is accomplished in the report and, consequently, amplitude and phase information is attained. In addition, caustics are discussed. Caustics are envelopes of the ray systems and, thus, are surfaces which separate propagating and non-propagating (or complex evanescent) regions and characterize the modal ray systems in non-uniform regions. The report concludes with a discussion of the transition region between the cylinder and the cone.

TABLE OF CONTENTS

LIST OF FIGURES

1. INTRODUCTION

The ray-optical method has provided physically meaningful results and a convenient approach for studying electromagnetic and acoustic problems in both the time and frequency domains [1,2,3]. A major contribution of the method is the insight it gives to problems inaccessible by other means. In attempting to determine the wave phenomena associated with a waveguide and antenna integrated structure consisting of a dielectric cylinder and cone, difficulty in analysis is immediately encountered because of the non-uniform geometry involved.

In studying the two-dimensional analogue--a dielectric slab feeding a dielectric wedge--it was found advantageous to determine ray solutions [4]. They, subsequently, were helpful in postulating a general plane wave integral representation for the field structure in the wedge region. Consequently, in order to gain insight into propagation and diffraction effects taking place for the cylinder-cone configuration, a ray-optical analysis was undertaken.

In Section 2, the method of geometrical optics is presented. The eiconal and transport equations are derived. Asymptotic boundary conditions are discussed and a generalized reflection coefficient introduced. Before investigating the cylinder-cone non-separable geometry, an understanding of the ray structure in both an infinite dielectric cylinder and, separately, in an infinite dielectric cone is needed. This is accomplished in Sections 3 and 4, respectively. Therein, amplitude and phase information is attained and caustics discussed. Caustics are surfaces which

separate propagating and non-propagating (or complex evanescent) regions and, as has been shown [2], characterize the modal ray systems in non-uniform regions. Finally, Section 5 provides some insight into the transition region between the cylinder and the cone.

2. FORMULATION AND RAY OPTICS

An integrated structure of dielectric cylindrical waveguide (of circular cross-section) feeding a cone of the same material is assumed to be excited by a source to the left (see Fig. 1). Field components in the dielectric can be deduced from a scalar wave function Ψ [5], which satisfies the reduced wave equation

$$(\nabla^2 + k^2)\, \Psi(\underline{r}) = 0 \tag{2.1}$$

with $k = \omega \sqrt{\mu_o \varepsilon_o \varepsilon_r}$, the wavenumber of a homogeneous lossless dielectric of relative dielectric constant ε_r. A time dependence of exp ($-i\omega t$) is assummed and suppressed. To obtain a unique solution to Eq. (2.1), either the tangential electric and magnetic fields at the air-dielectric surfaces must be continuous or the tangent electric field on the boundary must be linearly related to the tangent magnetic field (the so-called "impedance boundary condition"). This latter boundary condition can be expressed in terms of the scalar wave function Ψ by the relation

$$-ik\, \Psi(\underline{r}) + f(\underline{r})\, \frac{\partial \Psi(\underline{r})}{\partial \nu} = 0 \qquad \text{on B} \tag{2.2}$$

where ν is the outward normal to the boundary surface B, $f(\underline{r})$ is related to a surface impedance, and $\Psi(\underline{r})$ represents the solution to (2.1). For an infinite dielectric cylindrical waveguide, impedance boundary conditions* $E_z = -Z_{cy}^{(1)} H_\phi$ and $E_\phi = Z_{cy}^{(2)} H_z$ can be shown to reduce to (2.2) with $f(\underline{r})$ equal to a constant. For a conical dielectric structure, the conditions $E_r = -Z_{co}^{(1)} H_\phi$ and $E_\phi = Z_{co}^{(2)} H_r$ also can be shown to reduce to (2.2) but in this case $f = f(r)$ where r is the radial distance from the apex of the

*The quantities $(E_z, E_\phi, H_z, H_\phi)$ and $(E_r, E_\phi, H_r, H_\phi)$ are field components in cylindrical and spherical coordinates, respectively, whereas $Z_{cy}^{(i)}$, $Z_{co}^{(i)}$, i=1,2, are surface impedance functions.

cone. In obtaining (2.2) the assumption is made that Ψ varies as $\exp(-ik_z z)$, $\exp(ia\phi)$ where k_z and 'a' are separation constants, i.e., wave solutions to (2.1) are assumed to propagate forward the tip (in the -z direction) and to rotate in the $+\phi$ direction.

Following the development by Maurer and Felsen [2], a ray optics solution for large k of the form

$$\Psi(\underline{r}) \sim \sum_{p=1}^{N} A_p(\underline{r})\, e^{ik\, S_p(\underline{r})} \tag{2.3}$$

is assumed. Each species (denoted by p) has an amplitude, $A_p(\underline{r})$, assumed to be slowly varying, and a normalized phase $S_p(\underline{r})$. Inserting (2.3) into (2.1) and equating to zero the coefficients of the k^2 and of the k terms give, respectively,

$$\left(\nabla S_p(\underline{r})\right)^2 = 1 \tag{2.4}$$

and

$$2\, \nabla S_p(\underline{r}) \cdot \nabla A_p(\underline{r}) + A_p(\underline{r})\, \nabla^2 S_p(\underline{r}) = 0 \tag{2.5}$$

for any species p. Eqs. (2.4) and (2.5) are, respectively, the eiconal and transport equations of geometrical optics. Their solutions provide the amplitude and phase variations of the ray fields. It should be emphasized that ray solutions are only asymptotic expressions and are not full wave solutions. One way of examining the accuracy of a ray solution is to compare it with the asymptotic form of a full wave solution. This will be done for the cylindrical guide in Section 4.

Substituting the ray solution (2.3) into the boundary condition (2.2) yields

$$\sum_{p=1}^{N} e^{ik S_p(\underline{r})} A_p(\underline{r}) \left(-1 + f(\underline{r}) \frac{\partial S_p(\underline{r})}{\partial \nu} \right) = 0 \qquad (2.6)$$

Eq. (2.6) can be satisfied by postulating the pairwise vanishing of terms so that

$$e^{ik S_p} \left[A_p \right] \left[f(\underline{r}) \frac{\partial S_p}{\partial \nu} - 1 \right] + e^{ik S_q} \left[A_q \right] \left[f(\underline{r}) \frac{\partial S_q}{\partial \nu} - 1 \right] = 0$$

$$\text{on } B \qquad (2.7)$$

Equating phases of the exponential terms in (2.7) yields

$$k S_p = k S_q + 2\Pi m \qquad \text{on } B, \qquad (2.8)$$

where m is an integer such that initially $\frac{2m\Pi}{k}$ is of order 1. From the eiconal equation (2.4) and boundary condition (2.8), it can be shown that

$$\frac{\partial S_p}{\partial \nu} = - \frac{\partial S_q}{\partial \nu} \qquad \text{on } B \qquad (2.9)$$

The minus sign enters into the above equation because reflection takes place at the boundary. Using eqs. (2.8) and (2.9) in (2.7) gives

$$A_q = \Gamma A_p \qquad \text{on } B \qquad (2.10a)$$

where

$$\Gamma = \frac{f(\underline{r}) \frac{\partial S_p}{\partial \nu} - 1}{f(\underline{r}) \frac{\partial S_p}{\partial \nu} + 1} \qquad (2.10b)$$

Γ is recognized as a reflection coefficient.

If the reflection coefficient is constant on the boundary B, it is possible to construct an alternative formulation without destroying the specular reflection condition (2.9). In this formulation, the phase of Γ is incorporated into the phase function S rather than totally associated with amplitude terms as was done in (2.10). Rewriting (2.7) in the form

$$A_q e^{ik S_q} = A_p \Gamma e^{ik S_p} = A_p |\Gamma| e^{i \arg\Gamma + ik S_p}, \tag{2.11}$$

with Γ defined by (2.10b), leads naturally to the relations

$$A_q = A_p |\Gamma|, \quad k S_q = k S_p + \arg \Gamma - 2m\Pi. \tag{2.12}$$

If, furthermore, $|\Gamma| = 1$, then $\arg \Gamma = -i \ell n \Gamma$ and (2.12) reduces to

$$A_p = A_q , \tag{2.13a}$$

$$k S_p = k S_q + i \ell n \Gamma + 2m\Pi \tag{2.13b}$$

where m is an integer.

The solutions of eqs. (2.4) and (2.5), subject to appropriate boundary conditions [(2.10), (2.12) or (2.13)] in a given structure, is the subject of the next section. Before proceeding, it ought to be pointed out that the scalar wave function Ψ will be shown to be proportional to the longitudinal component E_z in the cylinder and to the radial component E_r in the cone.

3. RAY OPTICAL SOLUTIONS FOR DIELECTRIC CYLINDER AND CONE

The ray equations developed in Section 2 are now applied first to the infinite dielectric cylinder and then to the infinite dielectric cone. The asymptotic solution to the wave equation for the cylinder is found by solving the eiconal and transport equations in cylindrical coordinates subject to appropriate boundary conditions. A similar result is achieved for the cone using spherical coordinates.

When solutions to the eiconal equation are real, directions ∇S_p describe the modal-ray trajectories which satisfy the specular reflection law at boundaries. However, when phase functions $S_p(\underline{r})$ and ∇S_p become complex, real space trajectories cannot be defined. Surfaces which separate regions of space wherein the phase function S_p is either real or complex evanescent are called caustics. It will shortly become evident that caustics play a dominant role in the description of the ray structure in both the dielectric cylinder and cone. From knowledge of these phase functions in both geometries, reflection coefficients will be determined.

A. DIELECTRIC CYLINDER

a. Eiconal Equation

Since the geometry of an infinite dielectric guide is cylindrical, cylindrical coordinates are used (see Fig. 1). Following the procedure developed for two-dimensional configurations [2], the phase function of an arbitrary ray guided by the cylinder is assumed to have the separable form

$$S(\rho,\phi,z) = R(\rho) + \Phi(\phi) + Z(z) \tag{3.1}$$

Applying (2.4) yields

$$R'^2 + \frac{1}{\rho^2}\ \Phi'^2 + Z'^2 \ = \ \ 1,$$

where the prime denotes differentiation with respect to the argument. Rearranging terms gives

$$\Phi'^2 = -\rho^2\ (R'^2 + Z'^2 - 1). \tag{3.2}$$

Setting both sides of the above equation equal to a constant 'a' yields

$$\begin{aligned} \Phi'^2 &= a^2 \\ 1 - Z'^2 &= R'^2 + a^2/\rho^2 \end{aligned} \tag{3.2a}$$

Equating both sides of the latter equation to a second separation constant (or eigenvalue) 'b' results in

$$Z' = \pm \sqrt{1 - b^2} \tag{3.2b}$$

$$R' = \pm \sqrt{b^2 - a^2/\rho^2} \tag{3.2c}$$

Integrating eqs. (3.2) is straightforward and gives, ignoring the additive integration constants for a moment,

$$\begin{aligned} \Phi(\phi) \ &= \pm\ a\phi \\ Z(z) &= \pm \sqrt{1 - b^2}\ z \ = \pm\ \hat{Z}(z) \\ R(\rho) \ &= \pm[(\rho^2 b^2 - a^2)^{\frac{1}{2}} - a\ \cos^{-1}\ (a/b\rho)] \ = \pm\ \hat{R}(\rho) \end{aligned} \tag{3.3}$$

Combining (3.3) with (3.1) and introducing a composite integration constant explicitly, gives phase functions

$$S(\rho,\phi,z) = \pm \left[(\rho^2 b^2 - a^2)^{\frac{1}{2}} - a \cos^{-1}(a/b\rho)\right] \pm a\phi \pm \sqrt{1 - b^2}\, z + c \qquad (3.4)$$

Phase fronts S = constant progress along ray trajectories defined by the unit vector

$$\nabla S = \pm \sqrt{b^2 - a^2/\rho^2}\ \hat{\underline{a}}_\rho \pm (a/\rho)\, \hat{\underline{a}}_\phi \pm \sqrt{1 - b^2}\, \hat{\underline{a}}_z \qquad (3.5)$$

where $\hat{\underline{a}}_i$, $i = \rho,\phi,z$, are unit vectors along the coordinate axes. From (2.4), eight distinct phases are possible and are designated

$$\begin{aligned}
S_{1,2} &= \pm \hat{R}(\rho) + a\phi - \hat{Z}(z) + C_{1,2} \\
S_{3,4} &= \pm \hat{R}(\rho) - a\phi - \hat{Z}(z) + C_{3,4} \\
S_{5,6} &= \pm \hat{R}(\rho) + a\phi + \hat{Z}(z) + C_{5,6} \\
S_{7,8} &= \pm \hat{R}(\rho) - a\phi + \hat{Z}(z) + C_{7,8}
\end{aligned} \qquad (3.6)$$

where $\hat{R}(\rho)$ and $\hat{Z}(z)$ are taken as the positive signed quantities in (3.3).

b. Reflection Coefficient

Observing that the ρ-direction is normal to a cylindrical surface and assuming again that species p reflects into species q at the boundary $\rho = \rho_{cyl}$, (3.5) establishes that

$$\frac{\partial S_p}{\partial \nu} = \hat{\underline{a}}_\rho \cdot \nabla S = \sqrt{b^2 - \left(\frac{a}{\rho}\right)^2}$$

It follows on using (2.10b) that

$$\Gamma_{cyl} = \frac{f_{cyl}(\underline{r})\ \sqrt{b^2 - \left(\frac{a}{\rho}\right)^2} - 1}{f_{cyl}(\underline{r})\ \sqrt{b^2 - \left(\frac{a}{\rho}\right)^2} + 1} \quad \text{at } \rho = \rho_{cyl} \qquad (3.7)$$

The boundary of a cylinder is characterized by a constant ρ-value. Since the guide is rotationally symmetric and infinitely long, the parameter $f_{cyl}(\underline{r})$ and therefore the reflection coefficient Γ_{cyl} are assumed to be independent of the ϕ- and z-coordinates. A rigorous justification follows by referring to the exact modal solution presented in Section IV. If it is also assumed that rays are totally reflected at the dielectric-air interface, the absolute value of the reflection coefficient is unity and boundary conditions (2.13) apply. Thus, cylindrical ray amplitudes are not altered by reflection at the boundary ($A_p = A_q$ from (2.13a)). Furthermore, since the rays obey the specular law of reflection and Snell's law of refraction, it follows, for example, that rays progressing in the $(+\rho,+\phi\ ,\ +z)$-direction will reflect off the boundary in the $(-\rho,\ +\phi,\ +z)$-direction. In other words, ray specie S_1 will reflect into ray specie S_2, S_3 into S_4, S_5 into S_6, and S_7 into S_8. This reflection property of ray pairs at the cylinder walls is needed for solving the transport equation.

c. Transport Equation

The complex amplitude of a ray is given by the solution of the transport equation, eq. (2.5). Restricting our consideration for the moment to ray species S_1 and S_2 in (3.6) and referring to (3.4) and (3.5), the transport equation in cylindrical coordinates can be shown to take the form

$$\pm 2\sqrt{b^2 - a^2/\rho^2}\frac{\partial A_{1,2}}{\partial \rho} + 2\frac{a}{\rho}\frac{\partial A_{1,2}}{\partial \phi} - 2\sqrt{1 - b^2}\frac{\partial A_{1,2}}{\partial z} \pm \frac{b^2}{\sqrt{b^2\rho^2 - a^2}} = 0 \qquad (3.8)$$

where A_1 and A_2 are the ray amplitudes associated with phases S_1 and S_2. To solve (3.8), a product separable form

$$A = \tilde{R}(r)\tilde{\Phi}(\phi)\tilde{Z}(z)$$

can be assumed. Since an incident ray specie S_1 reflects off the dielectric-air boundary into a ray specie S_2, boundary conditions (2.13) stipulate that $A_1 = A_2$ at $\rho = \rho_{cy}$, where ρ_{cy} is the radius of the dielectric guide. Imposing the additional constraints that the field must be rotationally symmetric with regard to ϕ and must be bounded on the infinite z-domain while recalling that amplitude (as well as phase) changes along a ray trajectory are real, it can be shown that the amplitudes A_1 and A_2 are independent of ϕ and z. Hence, (3.8) reduces to

$$2\sqrt{b^2 - a^2/\rho^2}\ \frac{dA_i}{d\rho} + \frac{b^2}{\sqrt{b^2\rho^2 - a^2}} = 0, \qquad i = 1,2,$$

which has solutions

$$A_i(\rho) = K_{cyl}\ (2b^2\rho^2 - 2a^2)^{-1/4}, \qquad i = 1,2, \qquad (3.9)$$

where K_{cyl} is a constant. Eq. (3.9) has the expected $\rho^{-1/2}$ variation which is characteristic of cylindrical wave functions.

d. Caustics

Caustics are found by examining when real ray trajectories ∇S become complex. From (3.5), trajectories are real when $\rho > a/b$ and $b < 1$, i.e., $\rho > a/b > a$. If, however, either one of these conditions is violated, phase functions become complex and evanescent behavior results. Thus, in

a cylindrical waveguide, caustics are cylindrical surfaces of radii (see Fig. 2).

$$\rho_{ca} = a/b, \qquad b \leqslant 1. \tag{3.10}$$

Hence, for rays to propagate down a cylindrical guide of radius ρ_{cy},

$$\rho_{ca} < \rho_{cy} \tag{3.11}$$

e. Boundary conditions

It has already been noted that the direction rays travel down the guide is altered by reflection from the cylindrical boundary $\rho = \rho_{cy}$. In particular (see Fig. 2), S_1-rays, which proceed in the $(+\rho, +\phi, -z)$-direction, reflect at the boundary into S_2-rays, which progress in the $(-\rho, +\phi, -z)$-direction. Appropriate boundary conditions are prescribed in Eqs. (2.10), (2.12), or (2.13). This surface, however, is not the only boundary which affects the rays. All rays are tangent to caustics and upon traversing them experience a phase lag of ninety degrees. Thus,

$$k\, S_1 = k\, S_2 - \Pi/2 \quad \text{at} \quad \rho = \rho_{ca} \tag{3.12}$$

Using the expressions for S_1 and S_2 given in (3.6) and applying (3.12) gives

$$k\,(C_2 - C_1) = \Pi/2 \tag{3.13}$$

after noting that $\hat{R}(\rho_{ca})$ is zero. Letting $C_1 = -C_2$, as is done in [2], results in

$$k\, C_1 = -k\, C_2 = -\Pi/4 \tag{3.14}$$

Combining (3.14) with S_1 and S_2 in (3.6) gives

$$\begin{aligned} S_1 &= \hat{R}(\rho) + a\phi - \hat{Z}(z) - \Pi/4k \\ S_2 &= -\hat{R}(\rho) + a\phi - \hat{Z}(z) + \Pi/4k \end{aligned} \tag{3.15}$$

where $\hat{R}$ and $\hat{Z}$ are defined in (3.3).

Since the field structure must be rotationally invariant, the phase must satisfy the condition

$$S(\rho,\phi,z) = S(\rho,\phi + 2\Pi,z)$$

The phase dependence $\exp(\pm ika\phi)$ then requires that

$$ka = n, \qquad n = \text{integer} \tag{3.16}$$

Application of (2.13), with $S_{1,2}$ defined in (3.15), $C_{1,2}$ related by (3.13), and $ka = n$, yields the asymptotic modal equation for the eigenvalue $b = b_{mn}$

$$2\, k\, \hat{R}_{mn}(\rho_{cy}) = (2m + \tfrac{1}{2})\Pi + i\, \ell n \Gamma \quad , \tag{3.17}$$

where

$$k\hat{R}_{mn}(\rho_{cy}) = \sqrt{(kb_{mn}\rho_{cy})^2 - n^2} - n \cos^{-1}(n/kb_{mn}\rho_{cy})$$

f. The Mode Function

Modal fields in the cylindrical waveguide, which propagate in the $(-z, +\phi)$-direction, can now be constructed by the superposition of the S_1 and S_2 by

$$\Psi_{mn} \sim A_1 e^{ikS_1} + A_2 e^{ikS_2} \tag{3.19}$$

The phase functions $S_{1,2}$ are prescribed in (3.15) with eigenvalues a and b stipulated by (3.16) and (3.17). The amplitudes $A_{1,2}$ have been shown to be equal and to be functions only of ρ in (3.9). Thus, modal ray fields are

$$\Psi_{mn} = \frac{K_{cyl}}{(2b^2\rho^2 - 2a^2)^{1/4}} \cos\left[k\sqrt{\rho^2 b^2 - a^2} - ka\cos^{-1}\left(\frac{a}{b\rho}\right) - \pi/4\right]$$

$$\cdot e^{i\left[ka\phi - k(1-b^2)^{1/2} z\right]} \tag{3.20}$$

where K_{cyl} is a constant.

B. CONE

a. Eiconal Equation

Fig. 2 shows the dielectric cone with the appropriate spherical geometry. It is assumed that the phase is separable and has the form

$$S(r,\theta,\phi) = R_c(r) + \Theta(\theta) + \Phi_c(\phi) \tag{3.21}$$

In spherical coordinates, the eiconal equation (2.4) becomes

$$[R_c'^2 + \frac{1}{r^2}\,\textcircled{H}'^2 - 1][-r^2 \sin^2\theta] = \Phi_c'^2$$

Each side of the above equation is set equal to a separation parameter, called a_c^2, so that

$$\Phi_c'^2 = a_c^2 \quad , \qquad \Phi_c(\phi) = \pm a_c \phi \tag{3.22}$$

and

$$[-r^2][R_c'^2 - 1] = \frac{a_c^2}{\sin^2\theta} + \textcircled{H}'^2 \quad .$$

A second separation constant, b_c^2, is introduced such that

$$[-r^2][R_c'^2 - 1] = b_c^2 \qquad \text{and} \qquad \textcircled{H}'^2 + \frac{a_c^2}{\sin^2\theta} = b_c^2 \quad .$$

The first equation reduces to

$$R_c(r) = \pm\int\sqrt{1 - (\frac{b_c}{r})^2}\ dr = \pm\left[\sqrt{r^2 - b_c^2} - b_c \cos^{-1}[\frac{b_c}{r}]\right] \tag{3.23}$$

while the second reduces to the more complicated integral

$$\textcircled{H} = \pm \int \left(b_c^2 - \frac{a_c^2}{\sin^2\theta}\right)^{\frac{1}{2}} d\theta = a_c \int \frac{(C_c^2 \sin^2\theta - 1)^{\frac{1}{2}}}{\sin\theta} d\theta$$

$$= a_c \left[C_c^2 \int \frac{\sin\theta \, d\theta}{[C_c^2 \sin^2\theta - 1]^{\frac{1}{2}}} - \int \frac{d\theta}{\sin\theta \, [C_c^2 \sin^2\theta - 1]^{\frac{1}{2}}} \right],$$

where $C_c = b_c/a_c$.

The latter two integrals were found in Gradshteyn and Ryzhik [6] and subsequently evaluated with the result that

$$\textcircled{H}(\theta) = \pm \left[a_c \tan^{-1}\left(\frac{\cos\theta}{\sqrt{(b_c^2/a_c^2)\sin^2\theta - 1}} \right) - b_c \sin^{-1}\left(\frac{b_c \cos\theta}{\sqrt{b_c^2 - a_c^2}} \right) \right] \quad (3.24)$$

Combining (3.22), (3.23) and (3.24) with (3.21) expresses the phases of the conical rays as

$$S(r,\theta,\phi) = \pm \hat{R}_c(r) \pm \hat{\textcircled{H}}(\theta) \pm a_c\phi + C \ , \quad (3.25)$$

where C represents a composite integration constant,

$$\hat{R}_c(r) = \sqrt{r^2 - b_c^2} - b_c \cos^{-1}\left(\frac{b_c}{r}\right) \quad (3.26a)$$

$$\hat{H}(\theta) = a_c \tan^{-1}\left(\frac{\cos\theta}{\sqrt{(b_c^2/a_c^2)\sin^2\theta - 1}}\right) - b_c \sin^{-1}\left(\frac{b_c \cos\theta}{\sqrt{b_c^2 - a_c^2}}\right) \quad (3.26b)$$

and modal-ray trajectories are described by

$$\nabla S = \pm\sqrt{1 - (\frac{b_c}{r})^2}\,\hat{a}_r \pm \frac{1}{r}\sqrt{b_c^2 - (\frac{a_c}{\sin\theta})^2}\,\hat{a}_\theta \pm \frac{a_c}{r\sin\theta}\,\hat{a}_\phi \quad . \quad (3.27)$$

Eq. (3.27) can readily be shown to satisfy the eiconal equation (2.4). As in the cylinder, there are eight ray species in the cone which are defined by the phase functions

$$\begin{aligned}
S_{9,10} &= \pm \hat{R}_c(r) + \hat{H}(\theta) + a_c\phi + C_{9,10} \\
S_{11,12} &= \pm \hat{R}_c(r) - \hat{H}(\theta) + a_c\phi + C_{11,12} \\
S_{13,14} &= \pm \hat{R}_c(r) + \hat{H}(\theta) - a_c\phi + C_{13,14} \\
S_{15,16} &= \pm \hat{R}_c(r) - \hat{H}(\theta) - a_c\phi + C_{15,16}
\end{aligned} \quad (3.28)$$

where $\hat{R}$ and $\hat{H}$ are defined in (3.26).

b. Reflection Coefficient

Assuming a ray species p reflects into a species q, eq. (3.27) shows that the normal derivative of the phase S_p at a conical surface,

$$\frac{\partial S_p}{\partial \nu} = \hat{\underline{a}}_\theta \cdot \nabla S = \frac{1}{r} \sqrt{b_c^2 - \left(\frac{a_c}{\sin\theta}\right)^2} \ ,$$

depends on both r- and θ-coordinates. Thus, as defined in (2.10b) with $f_{co}(\underline{r})$, the reflection coefficient,

$$\Gamma_{cone} = \frac{f_{co}(\underline{r}) \frac{1}{r} \sqrt{b_c^2 - \left(\frac{a_c}{\sin\theta}\right)^2} - 1}{f_{co}(\underline{r}) \frac{1}{r} \sqrt{b_c^2 - \left(\frac{a_c}{\sin\theta}\right)^2} + 1} \qquad \text{at } \theta = \theta_{co}, \quad (3.29)$$

unlike the cylinder reflection coefficient (3.7), is not constant on the boundary of the dielectric cone (which is described by $\theta = \theta_{co}$ = constant). Thus, asymptotic boundary conditions are not applicable. Note, however, that symmetry implies that the surface impedance and therefore the reflection coefficient are independent of the ϕ-coordinate. This implies that ray amplitudes might also not vary with ϕ, a conjecture which proves fruitful in the following analysis of the transport equation.

c. *Transport Equation*

In the spherical coordinate system, the transport equation (2.5) involves the gradient

$$\nabla A = \frac{\partial A}{\partial r}\,\hat{a}_r + \frac{1}{r}\frac{\partial A}{\partial \theta}\,\hat{a}_\theta + \frac{1}{r \sin\theta}\,\frac{\partial A}{\partial \phi}\,\hat{a}_\phi$$

and the scalar Laplacian

$$\nabla^2 S = \frac{1}{r^2}\,\frac{\partial}{\partial r}\left(r^2 \frac{\partial S}{\partial r}\right) + \frac{1}{r^2 \sin\theta}\,\frac{\partial}{\partial \theta}\left(\sin\theta \frac{\partial S}{\partial \theta}\right) + \frac{1}{r^2 \sin^2\theta}\,\frac{\partial^2 S}{\partial \phi^2}$$

For the cone configuration (Fig. 3), rays progressing toward the boundary $\theta = \theta_{co}$ in the $(-r, +\theta, +\phi)$ direction reflect into rays progressing in the $(-r, -\theta, +\phi)$-direction. These ray families are represented in (3.28) by phase functions S_{10} and S_{12}, respectively. The associated ray paths are described by

$$\nabla S_{10,12} = -\sqrt{1 - \left(\frac{b_c}{r}\right)^2}\,\hat{a}_r \pm \frac{1}{r}\sqrt{b_c^2 - \left(\frac{a_c}{\sin\theta}\right)^2}\,\hat{a}_\theta + \frac{a_c}{r \sin\theta}\,\hat{a}_\phi \qquad (3.30)$$

The transport equation governing the amplitude behavior A_{10} and A_{12} corresponding to phases S_{10} and S_{12}, respectively, become on assuming no variation with ϕ because of rotational symmetry

$$2r^2\sqrt{1-\left(\frac{b_c}{r}\right)^2}\ \frac{\partial A_c}{\partial r} \mp \frac{2\sqrt{b_c^2\sin^2\theta - a_c^2}}{\sin\theta}\ \frac{\partial A_c}{\partial \theta} + \left[\frac{2r^2 - b_c^2}{\sqrt{r^2 - b_c^2}} \mp \frac{b_c^2\cos\theta}{\sqrt{b_c^2\sin^2\theta - a_c^2}}\right] A_c$$

$$= 0\ , \qquad (3.31)$$

where $A_c = A_{10}$ and $A_c = A_{12}$ correspond to the upper and lower signs, respectively.

To solve (3.31), the amplitudes are assumed to have the product separable form

$$A_c = \bar{R}(r)\ \bar{\Theta}(\theta) \qquad (3.32)$$

Substitution of (3.32) into (3.31) and introducing the separation constant α_c yield the differential equations

$$\frac{d\bar{R}}{dr} + \left[\frac{2r^2 - b_c^2 + \alpha_c\sqrt{r^2 - b_c^2}}{2r\,(r^2 - b_c^2)}\right]\bar{R} = 0 \qquad (3.34)$$

and

$$\frac{d\bar{\Theta}}{d\theta} + \frac{\left[b_c^2\cos\theta \pm \alpha_c\sqrt{b_c^2\sin^2\theta - a_c^2}\right]\sin\theta}{2\,(b_c^2\sin^2\theta - a_c^2)}\ , \qquad (3.35)$$

where again the upper and lower signs correspond to A_{10} and A_{12}, respectively. Integrating and combining yields

$$A_c = \bar{R}(r)\,\bar{\bar{H}}(\theta) = \frac{K_{co}}{\left\{r^2(r^2 - b_c^2)\left[(b_c \sin\theta/a_c)^2 - 1\right]\right\}^{1/4}} \tag{3.36}$$

with

$$\alpha_c = 0$$

and constant K_{co}. The condition $\alpha_c = 0$ results on requiring the modal field solutions, and therefore the amplitudes, to be unique; a direct integration of (3.34) yields a multiplicative factor $\exp\left[-(\alpha_c/2\,b_c)\sec^{-1}(r/b_c)\right]$ which is multivalued due to the presence of the secant function and thus requires $\alpha_c = 0$ for uniqueness. Observe that cone ray amplitudes have the familiar r^{-1} variation which appears in spherical wave functions.

d. Caustics

Caustic surfaces are determined from (3.27). It is clear that solutions are real for $\sin\theta \geq \frac{a_c}{b_c}$, $r \geq b_c$ and imaginary when either of these conditions is violated. There are therefore two caustics, a sphere

$$r = b_c \tag{3.37a}$$

e. Boundary Conditions

It has been observed that rays incident on the conical boundary ($\theta = \theta_{co}$) in the $(-r, +\theta, +\phi)$-direction are characterized by the phase S_{10} and reflect into the $(-r, -\theta, +\phi)$-direction associated with the phase S_{12} (see Fig. 3). Boundary condition (2.8) is therefore satisfied and specifies that

$$k\, S_{10} = k\, S_{12} + 2m\Pi \qquad \text{at } \theta = \theta_{co} \tag{3.39}$$

Boundary condition (2.13), which is used to study the reflection of rays from the cylindrical boundary, cannot be used for conical rays because the reflection coefficient (3.29) is not constant at $\theta = \theta_{co}$.

Fig. 3 also depicts an S_{12}-ray progressing toward the conical caustic ($\theta = \theta_{ca}$) with an S_{10}-ray leaving from a common tangent point. As was noted in (3.12), for rays tangent to a cylindrical caustic, S_{10} and S_{12} at the conical caustic experience a ninety-degree phase change stipulated by

$$k\, S_{10} = k\, S_{12} - \frac{\Pi}{2} \qquad \text{at } \theta = \theta_{ca} \tag{3.40}$$

While this formulation was complete in the cylinder, it is not in the cone. The spherical caustic $r = b_c$ serves as a reflecting boundary. We then are forced to consider rays travelling toward the tip, in one polarization, which bounce off the spherical caustic. A look at Fig. 4 indicates that rays incident in the $(-r, -\theta, +\phi)$-direction will be reflected from the spherical caustic in the $(+r, -\theta, +\phi)$-direction. Thus, at the spherical caustic, we have the following conditions (see (3.27)):

$$k\,S_9 = k\,S_{10} - \frac{\Pi}{2}$$

$$\text{at } r = b_c \tag{3.41}$$

$$k\,S_{11} = k\,S_{12} - \frac{\Pi}{2}$$

Furthermore, S_9-and S_{11}-rays couple at both the boundary and conical caustic (see Fig. 4) so that

$$k\,S_9 = k\,S_{11} - \frac{\Pi}{2} \qquad \text{at } \theta = \theta_{ca} \tag{3.42}$$

$$k\,S_{11} = k\,S_9 + 2m\Pi \qquad \text{at } \theta = \theta_{co} \tag{3.43}$$

f. Tangent Electric Field on Conical Surface

Determining the asymptotic expression for the modal field in the cone is more difficult than for the cylinder. This is largely due to the fact that the boundary condition required is (2.8) rather than (2.13b). If we consider rays propagating in the $(-z, +\phi)$-direction only, then the ray solution to the scalar wave equation in the cone takes the form

$$\Psi(\underline{r}) \sim A_{10}e^{ikS_{10}} + A_{12}e^{ikS_{12}}, \tag{3.44}$$

where A_{10} and A_{12} are specified by (3.36) with different constants and the phase functions S_{10} and S_{12} are given in (3.28). Instead of determining the modal field at arbitrary points in the dielectric cone, we will derive expressions for the tangent electric field at various points on its surface. This field is important because tangent fields are needed to formulate an integral expression for the far field. The tangential magnetic field follows in a similar fashion, but will not be discussed.

It is necessary at this point to relate the scalar wave function Ψ

given by (3.44) to the electromagnetic field. In a spherical coordinate system, the solution to Maxwell's source-free equations can be expressed in terms of two potential functions, $\underline{A} = \hat{\underline{r}}A$ and $\underline{F} = \hat{\underline{r}}F$. The associated wave functions $\Psi^a = A/r$ and $\Psi^f = F/r$ satisfy the reduced wave equation and field components are given by [5].

$$\underline{E} = -\nabla x\underline{F} - (1/i\omega\varepsilon)\nabla x\nabla x\underline{A} \tag{3.45a}$$

and

$$\underline{H} = \nabla x\underline{A} - (1/i\omega\mu)\nabla x\nabla x\underline{F} \tag{3.45b}$$

Noting that Ψ^a and Ψ^f satisfy the same wave equation, i.e. (2.1), we may write $\Psi^f = C_o\Psi^a$, where C_o is an arbitrary constant. For convenience, let incident and reflected wave functions be defined in terms of ray species S_{10} and S_{12}, respectively

$$\Psi^i \equiv A^i e^{ikS^i} = \Psi_{10} \equiv A_{10}e^{ikS_{10}} \tag{3.46a}$$

$$\Psi^r = A^r e^{ikS^r} = \Psi_{12} \equiv A_{12}e^{ikS_{12}} \tag{3.46b}$$

It follows that in spherical coordinates, the electric field components associated with these wave functions can be expressed, to order k, by

$$E^p_{ro}e^{ikS^p} = -i\eta kr\,[(\partial S^p/\partial r)^2 - 1]\,A^p e^{ikS^p} \tag{3.47a}$$

$$E^p_\theta = E^p_{\theta o}e^{ikS^p} = -i\eta k\left(\frac{\partial S^p}{\partial r}\right)\left(\frac{\partial S^p}{\partial \theta}\right)\,A^p e^{ikS^p} \tag{3.47b}$$

$$E^p_{\phi o}e^{ikS^p} = -i\eta k\,\frac{a_c(\partial S^p/\partial r)}{\sin\theta}\,A^p e^{ikS^p} \tag{3.47c}$$

where k and η are the wavenumber and intrinsic wave impedance of the dielectric cone and superscript p = i or r for incident or reflected field components, respectively.

The tangent electric field on the conical surface is expressed in terms of the asymptotic vector amplitudes $\underline{E}_o^{i,r}$ by

$$\underline{E}_{tan} = \hat{\underline{N}} \times (\underline{E}^i \times \underline{E}^r) \sim (\hat{\underline{N}} \times \underline{E}_o^i)\, e^{ikS^i} + (\hat{\underline{N}} \times \underline{E}_o^r)\, e^{ikS^r}, \qquad (3.48)$$

where the outward directed surface normal $\hat{\underline{N}} = \hat{\underline{\theta}}$. Following the development of Lewis and Keller [7], the amplitudes $\underline{E}_o^{i,r}$ are related to components both parallel and normal to the plane of incidence,* defined by the unit vectors ∇S^i and $\hat{\underline{N}}$ via the relations

$$\underline{E}_o^{i,r} = E_p^{i,r}\, \hat{\underline{V}}^{i,r} + E_n^{i,r}\, \hat{\underline{V}} \qquad (3.49)$$

with

$$\nabla S^r \times \hat{\underline{N}} = \nabla S^i \times \hat{\underline{N}} = (n_1 \sin w)\, \hat{\underline{V}}\,, \quad \hat{\underline{V}}^{i,r} = \hat{\underline{V}} \times \nabla S^{i,r}/n_1 \qquad (3.50)$$

The scalar amplitude components $E_p^{i,r}$ and $E_n^{i,r}$ and their associated unit vectors $\hat{\underline{V}}^{i,r}$ and $\hat{\underline{V}}$ are parallel and perpendicular to the plane of incidence, respectively. The index of refraction n_1 describes the dielectric material of the cone and w is the angle of incidence defined in Fig. 5.

Using the expressions [7]

$$\hat{\underline{N}} \times \underline{E}_o^i = E_p^i \cos w\ \hat{\underline{V}} + E_n^i\, \hat{\underline{N}} \times \hat{\underline{V}} \qquad (3.51a)$$

and

$$\hat{\underline{N}} \times E_o^r = -E_p^r \cos w\ \hat{\underline{V}} + E_n^r\, \hat{\underline{N}} \times \hat{\underline{V}} \qquad (3.51b)$$

the tangent electric field (3.48) becomes

---

*It can be shown that $\underline{E}^{i,r} \cdot \nabla S^{i,r} \simeq 0$ provided $r \gg b_c$

$$\underline{E}_{tan} = (E_p^i e^{ikS^i} - E_p^r e^{ikS^r})\,\hat{\underline{V}}\cos w - (E_n^i e^{ikS^i} + E_n^r e^{ikS^r})\,\hat{\underline{V}} \times \hat{\underline{N}} \tag{3.52}$$

1. A single reflection from the conical air-dielectric interface

As the rays progress in the conical radiator toward the tip, their amplitudes are altered by Fresnel polarization dependent reflection coefficients [7]

$$\Gamma_p \equiv E_p^r/E_p^i \quad , \quad \Gamma_n \equiv E_n^r/E_n^i \qquad \text{at} \quad \theta = \theta_{co} \, , \tag{3.53}$$

which for $\mu_1 = \mu_2 = \mu_o$ are given by

$$\Gamma_p = \frac{\sqrt{\frac{1}{\varepsilon_r} - \sin^2 w} - \cos w}{\sqrt{\frac{1}{\varepsilon_r} - \sin^2 w} + \cos w} \quad , \quad \Gamma_n = \frac{\sqrt{\varepsilon_r - \varepsilon_r^2 \sin^2 w} - \cos w}{\sqrt{\varepsilon_r - \varepsilon_r^2 \sin^2 w} + \cos w} \tag{3.54a, 3.54b}$$

In addition, the incident and reflected phase terms satisfy the relation

$$kS^i = kS^r + 2m\Pi \qquad , \quad \theta = \theta_{co} \tag{3.55}$$

Applying boundary conditions (3.53) and (3.55) to (3.52), while considering surface points at which only one reflection takes place, yields

$$\underline{E}_{tan} = [E_p^i (1 - \Gamma_p)\,\hat{\underline{V}}\cos w - E_n^i (1 + \Gamma_n)\,\hat{\underline{V}} \times \hat{\underline{N}}]\; e^{ikS^i} \tag{3.56}$$

For (3.56) to be useful, relationships between the scalar amplitudes E_p^i, E_n^i and spherical components E_{ro}^i, $E_{\theta o}^i$, $E_{\phi o}^i$ in (3.47) must be established from (3.51a)

$$\hat{\underline{N}} \times \underline{E}_o^i = -E_{ro}^i\,\hat{\underline{\phi}} + E_{\phi o}^i\,\hat{\underline{r}} = E_p^i \cos w\,\hat{\underline{V}} + E_n^i\,\hat{\underline{N}} \times \hat{\underline{V}} \tag{3.57}$$

Using the definition of $\hat{\underline{V}}$ in (3.50), and noting that $\nabla S^i = \nabla S_{10}$ is given

in (3.30), the vector $\hat{\underline{V}}$ in spherical components becomes

$$\hat{\underline{V}} = [-(a_c/r \sin\theta)\,\hat{\underline{r}} + (1 - b^2{}_c/r^2)^{\frac{1}{2}}\,\hat{\underline{\phi}}]/n_1 \sin w \equiv [v_r\,\hat{\underline{r}} + v_\phi\,\hat{\underline{\phi}}]/\sin w \tag{3.58}$$

Recalling that $\hat{\underline{N}} = \hat{\underline{\theta}}$, it then follows from (3.58) that (3.57) yields the expressions

$$E^i_n = (v_\phi E^i_{\phi o} + v_r E^i_{ro}) \,/\, \sin w \tag{3.59a}$$

and

$$E^i_p = (v_r E^i_{\phi o} - v_\phi E^i_{ro}) \,/\, \sin w \cos w \tag{3.59b}$$

Thus, the tangential electric field on the conical surface $\theta = \theta_{co}$, allowing for one reflection, is prescribed by (3.56) with unit vector $\hat{\underline{V}}$, Fresnel reflection coefficients and amplitude terms specified by (3.58), (3.53) and (3.59), respectively.

2. Multiple reflections from the conical air-dielectric boundary

As rays travel in the conical structure, they experience multiple reflections from the conical boundary. Each reflection introduces two angularly dependent Fresnel reflection coefficients (see (3.53)). The tangent electric field can be obtained at successive reflection points along the conical air-dielectric boundary by tracking a ray as it travels toward the apex of the cone (see Fig. 3) and introducing these two reflection coefficients each time the ray strikes the boundary.

Consider an observation point P_1 $(r_1, \theta_{co}, \phi_1)$ on the boundary $\theta = \theta_{co}$ as depicted in Fig. 3 and Fig. 6. For incidence angle w_1, it follows from (3.53) that

$$E^r_{p1} = \Gamma_{p1} E^i_{p1} \quad , \qquad E^r_{n1} = \Gamma_{n1} E^i_{n1} \tag{3.60}$$

At a second reflection point P_2 $(r_2, \theta_{co}, \phi_2)$ and for an angle of incidence w_2, E^r_{p1} and E^r_{n1} become E^i_{p2} and E^r_{p2}, respectively. Therefore, (3.53) and (3.60) specify that

$$E^r_{p2} = \Gamma_{p2} E^i_{p2} = \Gamma_{p1}\Gamma_{p2} E^i_{p1} \quad , \quad E^r_{n2} = \Gamma_{n2} E^i_{n2} = \Gamma_{n1}\Gamma_{n2} E^i_{n1} \tag{3.61}$$

By continuing the process of tracking reflections, we get at $P_\ell(r_\ell, \theta_{co}, \phi_\ell)$ and for $w^i = w_\ell$ a series representation of the form

$$E^i_{p,\ell} = \Gamma_{p1}\Gamma_{p2} \cdots \Gamma_{p,\ell-1} E^i_{p1} = \prod_{m=1}^{\ell-1} \Gamma_{p,m} E^i_p \tag{3.61a}$$

$$E^i_{n,\ell} = \Gamma_{n1}\Gamma_{n2} \cdots \Gamma_{p,\ell-1} E^i_{n1} = \prod_{m=1}^{\ell-1} \Gamma_{n,m} E^i_n \tag{3.61b}$$

where

$$\Gamma_{p,m} = \Gamma_p(w_m) \quad \text{and} \quad \Gamma_{n,m} = \Gamma_n(w_m) \tag{3.61c}$$

The incidence angles w_m are determined by tracking a ray as it travels in the conical radiator. Consider the construction in Fig. 6. Observe that the ray directions from P_o to P_{oc} is given by ∇S_{12} and from P_{oc} to P_1 by ∇S_{10}, which for convenience is repeated as follows

$$\nabla S_{\substack{10 \\ 12}} = -(1 - (b_c/r)^2)^{\frac{1}{2}}\, \hat{\underline{r}} \pm (1/r)(b_c^2 - (a_c/\sin\theta)^2)^{\frac{1}{2}}\, \hat{\underline{\theta}} + (a_c/r\sin\theta)\, \hat{\underline{\phi}} \tag{3.62}$$

The angle θ_o in Fig. 6 is found by taking the dot product of ∇S_{12} and $\hat{\underline{r}}$, and evaluating it at the point $P_o(r_o, \theta_{co}, \phi_o)$;

$$\cos\theta_o = \nabla S_{12} \cdot (-\hat{\underline{r}}) = (1 - (b_c/r_o)^2)^{\frac{1}{2}} \tag{3.63}$$

From geometrical construction in Fig. 6,

$$\theta_1 = \theta_o + 2\theta_{co} \tag{3.64}$$

$$r_1 = b_c/\sin\theta_1 \tag{3.65}$$

Since the angle of incidence w_1 is defined as the angle between the ray direction ∇S_{10} and the unit normal $\hat{\underline{N}} = \hat{\underline{\theta}}$ at $(r_1, \theta_{co}, \phi_1)$,

$$\cos w_1 = \nabla S_{10} \cdot \hat{\underline{\theta}} = (1/r_1)\ (b_c^2 - (a_c/\sin\theta)^2)^{\frac{1}{2}} \tag{3.66}$$

Using $a_c = b_c \sin\theta_{ca}$, (3.64) and (3.65), the above equation reduces to

$$\cos w_1 = \sin(\theta_o + 2\theta_{co})\ \ (1 - (\sin\theta_{ca}/\sin\theta_{co})^2)^{\frac{1}{2}} \tag{3.67}$$

which specifies w_1 in terms of the known parameters θ_{co}, θ_{ca} and θ_o. Following the above procedure, it becomes evident that the incident angle w_ℓ associated with a ray reaching the conical wall at the point P_ℓ after undergoing ℓ reflections is given by the similar expression

$$\cos w_\ell = \sin\theta_\ell\ \ (1 - (\sin\theta_{ca}/\sin\theta_{co})^2)^{\frac{1}{2}} \tag{3.68}$$

with

$$\theta_\ell = \theta_o + 2\ell\theta_{co} \tag{3.68a}$$

and θ_o specified by (3.63). In Section 4, continuity of the field at the transition region will be applied and relationships for the conical eigenvalues (a_c, b_c) will be found in terms of physical parameters.

Thus, after ℓ reflections from the conical air-dielectric interface, the surface tangential electric field at the point P_ℓ $(r_\ell, \theta_{co}, \phi_\ell)$ can be

inferred from (3.56) and by using (3.61) to be

$$\underline{E}_{tan,\ell} = [(\cos w_\ell) E_p^i (1 - \Gamma_{p,\ell}) \prod_{m=1}^{\ell-1} \Gamma_{p,m} \hat{\underline{V}}_\ell - E_n^i (1 + \Gamma_{n,\ell}) \prod_{m=1}^{\ell-1} \Gamma_{n,\ell} \hat{\underline{V}}_\ell \times \hat{\underline{\theta}}] e^{ikS_\ell^i} \tag{3.69}$$

where $\hat{\underline{V}}_\ell = \hat{\underline{V}}(r_\ell, \theta_{co}, w_\ell)$ is specified by (3.58), w_ℓ by (3.68) and S_ℓ^i by S_{10} in (3.28) evaluated at r_ℓ, θ_{co}, ϕ_ℓ. The ϕ-variation experienced by a ray as it proceeds toward the tip is illustrated in Fig. 7a and 7b.

4. COMPARISON OF RAY OPTICAL SOLUTION WITH EXACT MODAL SOLUTION IN THE CYLINDER

The expression for the guided modes of an infinite dielectric cylinder are well known [8]. The longitudinal electric field component, assuming propagation in the z-direction and suppressing the $\exp(-i\omega t)$ time dependence, is given within the cylinder ($\rho \leq \rho_{cyl}$) by

$$E_z = A\, J_n\,(k_t\,\rho)\; e^{\,in\phi \,-\, i\sqrt{k^2 - k_t^2}\; z} \tag{4.1}$$

Allowable eigenvalues k_t are prescribed by a rather complicated eigenvalue equation, which can be found in [8].

The Bessel function in (4.1) can be expressed in terms of the Hankel functions of the first and second kind of order n by

$$J_n\,(k_t\,\rho) = \frac{H_n^{(1)}\,(k_t\,\rho) + H_n^{(2)}\,(k_t\,\rho)}{2} \tag{4.2}$$

When $k_t\,\rho \to \infty$, the Hankel functions can be approximated by the (Debye) asymptotic forms

$$H^{(1)}_{k_t a_1}\,(k_t\,\rho) \sim \sqrt{\frac{2}{\pi k_t}}\,(\rho^2 - a_1^2)^{-\frac{1}{4}}\; e^{\,ik_t\,\left[(\rho^2 - a_1^2)^{\frac{1}{2}} - a_1 \cos^{-1}\left(\frac{a_1}{\rho}\right)\right] \,-\, i\frac{\pi}{4}} \tag{4.3}$$

$$H^{(2)}_{k_t a_1}\,(k_t\,\rho) \sim \sqrt{\frac{2}{\pi k_t}}\,(\rho^2 - a_1^2)^{-\frac{1}{4}}\; e^{\,-ik_t\,\left[(\rho^2 - a_1^2)^{\frac{1}{2}} - a_1 \cos^{-1}\left(\frac{a_1}{\rho}\right)\right] \,+\, i\frac{\pi}{4}}$$

where we have set $n = k_t a_1$. It should be pointed out that (4.3) are reasonably strong asymptotic expressions for Hankel functions in the sense that

they are not restricted to exceptionally large values of $k_t \rho$ but also apply to moderate values. Using (4.2) and (4.3) in (4.1), the asymptotic of the full wave solution becomes

$$E_z(\underline{r}) \simeq A_{F.W.} e^{ik_t a_1 \phi - i\sqrt{k^2 - k_t^2}\, z} \left[e^{ik_t R_{FW}(\rho) - i\frac{\Pi}{4}} + e^{-ik_t R_{FW}(\rho) + i\frac{\Pi}{4}} \right] \tag{4.4}$$

where

$$A_{FW} = \sqrt{\frac{2}{\Pi k_t}} \frac{A}{(\rho^2 - a_1^2)^{\frac{1}{4}}} \tag{4.4a}$$

and

$$R_{F.W.} = (\rho^2 - a_1^2)^{\frac{1}{2}} - a_1 \cos^{-1}\left(\frac{a_1}{\rho}\right) \tag{4.4b}$$

Since we are interested in the HE_{11} mode, $n = 1$ or $k_t a_1 = 1$. Hence,

$$a_1 = \frac{1}{k_t} \tag{4.5}$$

We now return to the ray-optic results. The scalar wave function given asymptotically by (3.20) is related to the electric field E_z via [5]

$$E_z = [k_t^2/(-iw\varepsilon)]\, \Psi \tag{4.6}$$

Hence,

$$E_z(\underline{r}) \simeq \frac{K'_{cyl}}{[2\, b^2\rho^2 - 2\, a^2]^{\frac{1}{4}}} e^{ika\phi - i\, k\sqrt{1 - b^2}\, z} \left[e^{i\,(k\,\hat{R}(\rho) + \frac{\Pi}{4})} + e^{-i\,(k\,\hat{R}(\rho) + \frac{\Pi}{4})} \right] \tag{4.7}$$

where

$$K'_{cyl} = K_{cyl}\, k_t^2 \,/\, (-jw\varepsilon) \tag{4.7a}$$

and

$$\hat{R}(\rho) = \sqrt{\rho^2 b^2 - a^2} - a \cos^{-1}\left(\frac{a}{b\rho}\right) \tag{4.7b}$$

A comparison can be first made between the phase factors in (4.4) and (4.7). From the ϕ dependence, $k_t a_1 = ka = 1$; hence,

$$a = \frac{1}{k} \tag{4.8}$$

From the z dependence,

$$k\sqrt{1 - b^2} = \sqrt{k^2 - k_t^2} = k\sqrt{1 - (\frac{k_t}{k})^2}$$

and therefore

$$b = \frac{k_t}{k} \tag{4.9}$$

If this ray solution is correct, the r-dependence must also agree. Thus, from (4.4) and (4.7)

$$k_t \, R_{FW}(\rho) = k \, \hat{R}(\rho). \tag{4.10}$$

From (4.4b) and (4.5)

$$k_t \, R_{FW}(\rho) = \sqrt{\rho^2 k_t^2 - 1} - \cos^{-1}\left[\frac{1}{\rho k_t}\right] \tag{4.11}$$

From (4.7b), (4.8) and (4.9), it follows that (4.10) is satisfied. Thus, the phase of the asymptotic of the full wave solution and the ray-optic solution are identical.

In matching the amplitudes, we note, using (4.5), that the asymptotic form of the amplitude of the full wave solution in (4.4a) takes the form

$$A_{FW} = A\sqrt{\frac{2}{\pi}} \, (\rho^2 \, k_t^2 - 1)^{-\frac{1}{4}} \tag{4.12}$$

Using (4.8) and (4.9), (4.12) reduces to

$$A_{FW} = A \sqrt{\frac{2}{\pi k}} \left(2 \rho^2 b^2 - 2 a^2\right)^{-1/4} 2^{1/4} \tag{4.13}$$

Comparison of (4.13) with amplitude terms of the ray solution (4.7) completes the identification. Since all fields in the guide can be expressed in terms of E_z, all asymptotic forms of field components of the exact modal solution in the cylindrical guide agree with their ray-optical counterparts.

Because of the above comparison, physical parameters are now associated with the separation constants a and b first introduced in (3.2). From (4.8) and (4.9) it evolved that $a = 1/k$ and $b = k_t/k$, where $k^2 = k_t^2 + k_z^2 = \omega^2 \mu_o \varepsilon_o \varepsilon_r$. For propagation in all directions, $k \geq k_t$; hence, $b = k_t/k \leq 1$, which agrees with (3.10). In addition, real ray solutions have been shown to be confined to the region (see (3.10) and (3.11))

$$\rho > \rho_{ca} = \frac{a}{b} = \frac{1}{k_t} \quad . \tag{4.14}$$

The asymptotic expression (4.4) also predicts propagation in this region.

5. TRANSITION REGION

As shown in Fig. 1, the transition region is defined as the region where the cylinder ends and the cone begins. It shall be assumed that the apex angle θ_{co} is small so that diffraction effects caused by this discontinuity in surface geometry can be ignored. The field across the transition must nonetheless be continuous. This means that the asymptotic field i.e., the rays must also be continuous; cylindrical rays must convert to conical rays on crossing the interface $r = r_T$, $\theta_{ca} \leq \theta \leq \theta_{co}$. To satisfy these conditions and to understand the wave phenomena involved, the ray direction in the cylinder, ∇S will be equated to the ray direction in the cone in the limit of small θ_{co}. This will yield solutions for the conical eigenvalues (a_c, b_c) in terms of cylindrical eigenvalues (a, b). Further checks on the continuity of rays across the transition region follow by investigating the continuity of reflection coefficients, caustics and the fields.

A. CONTINUITY OF RAY PATHS

We first notice from (3.4) and (3.25), that the ϕ dependence of the phase function in both the cylinder and cone are identical. Thus, we anticipate that

$$a = a_c \tag{5.1}$$

We now turn to ∇S in the cylinder (3.5) and in the cone (3.27). We propose to express the conical result in cylindrical coordinates by noting

the simple geometric identities

$$\hat{a}_z = \hat{a}_r \cos\theta - \hat{a}_\theta \sin\theta$$

$$\hat{a}_\rho = \hat{a}_r \sin\theta + \hat{a}_\theta \cos\theta \tag{5.2}$$

Since θ is very small, $\cos\theta >> \sin\theta$, and we approximate (5.2) by

$$\hat{a}_z \simeq \hat{a}_r \quad , \qquad \hat{a}_\rho \simeq \hat{a}_\theta \tag{5.3}$$

Hence, (3.27) becomes

$$\nabla S \simeq \sqrt{1 - \left(\frac{b_c}{r_T}\right)^2}\, \hat{a}_z + \frac{1}{r_T} \sqrt{b^2_c - \frac{a^2_c}{\sin^2\theta}}\, \hat{a}_\rho + \frac{a_c}{r_T \sin\theta} \hat{a}_\phi \tag{5.4}$$

Equation (5.4) is now compared with (3.5); equating coefficients of $\hat{a}_\phi$ and noting that $\rho_T = r_T \sin\theta$ gives $a_c = a$, which confirms (5.1). Matching $\hat{a}_z$ terms yields

$$b_c = b r_T \tag{5.5}$$

Using (5.1) and (5.5) in the $\hat{a}_\rho$ term of (5.4) agrees with the corresponding $\hat{a}_\rho$ term of (3.5), insuring continuity of ray paths.

B. REFLECTION COEFFICIENT

At surface transition points (r_T, θ_{co}, $0 \leq \phi \leq 2\pi$), reflection coefficients in the cylinder and cone must be approximately equal so that continuity of the ray fields is maintained. From (5.1) and (5.5), the reflection coefficient for the cone rays (3.29) becomes

$$\Gamma_{co} = \frac{f_{co}(\underline{r}_T)\sqrt{b^2 - (a/\rho_{cy})^2} - 1}{f_{co}(\underline{r}_T)\sqrt{b^2 - (a/\rho_{cy})^2} + 1} \tag{5.6}$$

which agrees with (3.7) provided

$$f_{co} = f_{cyl} \quad \text{at } r = r_T, \quad \theta = \theta_{co}, \quad 0 \leq \phi \leq 2\pi \tag{5.7}$$

C. CAUSTICS

We begin with an examination of the spherical caustic in the cone $r = b_c \equiv r_{ca}$. The radius of this caustic is related to r_T according to (5.5); hence,

$$r_{ca} = br_T \tag{5.8}$$

The parameter b is related to wavenumbers k and k_t by (4.9).

We must now verify that the radius of the conical caustic at (r_t, θ_{co}) equals the constant radius of the cylindrical caustic given by (4.14). We note from (3.37b) that the conical caustic is given by

$$\sin\theta_{ca} = \frac{a_c}{b_c} = \frac{a}{br_T} = \frac{1}{r_T k_t}$$

where use was made of (4.8) and (4.9), (5.1) and (5.5). Thus,

$$r_T \sin\theta_{ca} = \frac{1}{k_t} \tag{5.9}$$

From (4.14),

$$\rho_{ca} = \frac{1}{k_t} \quad \text{at the transition region} \tag{5.10}$$

Thus, the caustics connect continuously across the transition region

D. FIELD CONTINUITY

Since the tangent field on the conical surface was formulated in (3.69), a convenient way of insuring field continuity across the transition region is to match field components at the surface point (r_T, θ_{co}). The tangent electric field at this point is given by (3.56) which has two field components $E_r \equiv E_r^{co}$ and $E_\phi = E_\phi^{co}$. Hence, we can insist that at (r_T, θ_{co})

$$E_r^{cy} = E_r^{co} , \qquad E_\phi^{cy} = E_\phi^{co} \tag{5.11a}$$

and, similarly, that

$$H_r^{cy} = H_r^{co} , \qquad H_\phi^{cy} = H_\phi^{co} \tag{5.11b}$$

The superscripts clearly designate the field component as being associated with the cylinder or the cone. From geometrical considerations, we note that at (r_T, θ_{co})

$$E_r^{cy} = E_z^{cy} \cos\theta_{co} + E_\rho^{cy} \sin\theta_{co} , \quad H_r^{cy} = H_z^{cy} \cos\theta_{co} + H_\rho^{cy} \sin\theta_{co} \tag{5.12}$$

In Section 4 we have compared the asymptotic form of the exact solution for the electric field $E_z \equiv E_z^{cy}$ in the infinite dielectric cylinder with the ray optical solution (see eqs. (4.4) and (4.7)). The remaining field components follow from the expressions [8]

$$E_\rho^{cy} = \frac{-i}{k_t^2}\left[k_z \frac{\partial E_z}{\partial \rho} - \frac{\omega\mu_o}{\rho}\frac{\partial H_z}{\partial \phi}\right] , \quad E_\phi^{cy} = \frac{-i}{k_t^2}\left[\frac{k_z}{\rho}\frac{\partial E_z}{\partial \phi} + \omega\mu_o \frac{\partial H_z}{\partial \rho}\right] \tag{5.13a}$$

$$H_\rho^{cy} = \frac{-i}{k_t^2}\left[k_z \frac{\partial H_z}{\partial \rho} + \frac{\omega\varepsilon}{\rho}\frac{\partial E_z}{\partial \phi}\right] , \quad H_\phi^{cy} = \frac{-i}{k_t^2}\left[\frac{k_z}{\rho}\frac{\partial H_z}{\partial \phi} - \omega\varepsilon \frac{\partial E_z}{\partial \rho}\right] \tag{5.13b}$$

where the phase factor $\exp(-ik_z z)$, $k_z = (k^2 - k_t^2)^{1/2}$, has been suppressed

and H_z is proportional to E_z, i.e., $H_z = A_o E_z$ where A_o is known from continuity of the tangent fields across the cylinder air-dielectric interface [8]. Hence, since the field associated with the cylindrical waveguide is known to within a single constant, then by setting the constant A in (4.1) to unity and applying continuity of the tangent electric field (5.11a) at (r_T, θ_{co}), the unknown constant A^p and phase constant C^p in (3.46) or (3.47) can be found numerically. Continuity of the tangential magnetic field given by (5.11b) would then have to be checked.

6. SUMMARY AND SUGGESTIONS

The modal ray structure in a dielectric cylinder has been presented. Its validity was substantiated by a comparison of the longitudinal electric field component derived ray-optically with the asymptotic form of the exact modal solution. Ray species, trajectories, caustics as well as phase and amplitude variation of rays were all adequately explained. We next examined a dielectric conical structure and ascertained the ray description. The cylindrical caustic in the cylinder was seen to evolve continuously into a conical caustic in the cone. A spherical caustic was found centered at the cone's tip. Skew rays were carefully tracked in the cone and the surface tangential electric field was found asymptotically in terms of Fresnel polarization dependent reflection coefficients. Finally, a procedure was outlined for establishing field continuity across the transition region between the cylinder and the cone.

The above ray-optical treatment of the wave guidance of the integrated cylinder-cone structure is to be considered a first step in understanding the wave processes taking place. The next step, in analogy with our treatment of the dielectric slab waveguide-wedge antenna [4], is to formulate an integral representation for the surface field which asymptotically reduces to the above ray optical result in the transition region. A surface integration of this field will then enable us to find the radiation pattern of the cone.

7. ACKNOWLEDGEMENT

The authors wish to acknowledge the financial support provided for this project by the U.S. Army Research Office, Durham, North Carolina, and wish, in particular, to thank Dr. J. Mink for his continued interest and encouragement. Our appreciation is further extended to Dr. A. Allentuch, Dean of Research, at the New Jersey Institute of Technology, for his enthusiasm and for providing supplementary support. Special gratitude is due Dr. F. Schwering for his valuable discussions and advice throughout the progression of this study. Thanks is due Mr. J. Martinez, a former graduate student of the New Jersey Institute of Technology, for assistance in formulating the structure of the surface field on the cone.

8. REFERENCES

1. Keller, J. B., "A Geometric Theory of Diffraction," Calculus of Variations and its Applications, Symposia Appl. Math., Vol. 8, McGraw-Hill, New York, 1958.

2. Maurer, S.J. and Felsen, L.B., "Ray Optical Techniques for Guided Waves," Proceedings of the IEEE, Vol. 55, No. 10, Oct. 1967.

3. Whitman, G.M. and Felsen, L.B., "Pulse Propagation in a Dispersive Medium with Moving Density Profile," J. of Math. Physics, Vol. 13, pp. 760-768, 1972.

4. Whitman, G.M., Maurer, S.J., and Noerpel, A.R., "Radiation from Integrated Dielectric Millimeter-Wave Slab-Wedge Structures," prepared for the U.S. Army Research Office, N.C. under contract No. DAAG29-77-G-0094, New Jersey Institute of Technology Tech. Rept. , Oct. 1979.

5. Harrington, R.F., "Time-Harmonic Electromagnetic Fields," McGraw-Hill, New York, 1961.

6. Gradshteyn, I.S. and Ryzhik, I.M., "Table of Integrals, Series, and Products," Academic Press, New York, 1965.

7. Lewis, R.M. and Keller, J.B., "Asymptotic Methods for Partial Differential Equations: The Reduced Wave Equation and Maxwell's Equation," New York University, Rept. No. 5635.

8. Marcuse, D., "Light Transmission Optics," Van Nostrand Reinhold Co., 1972.

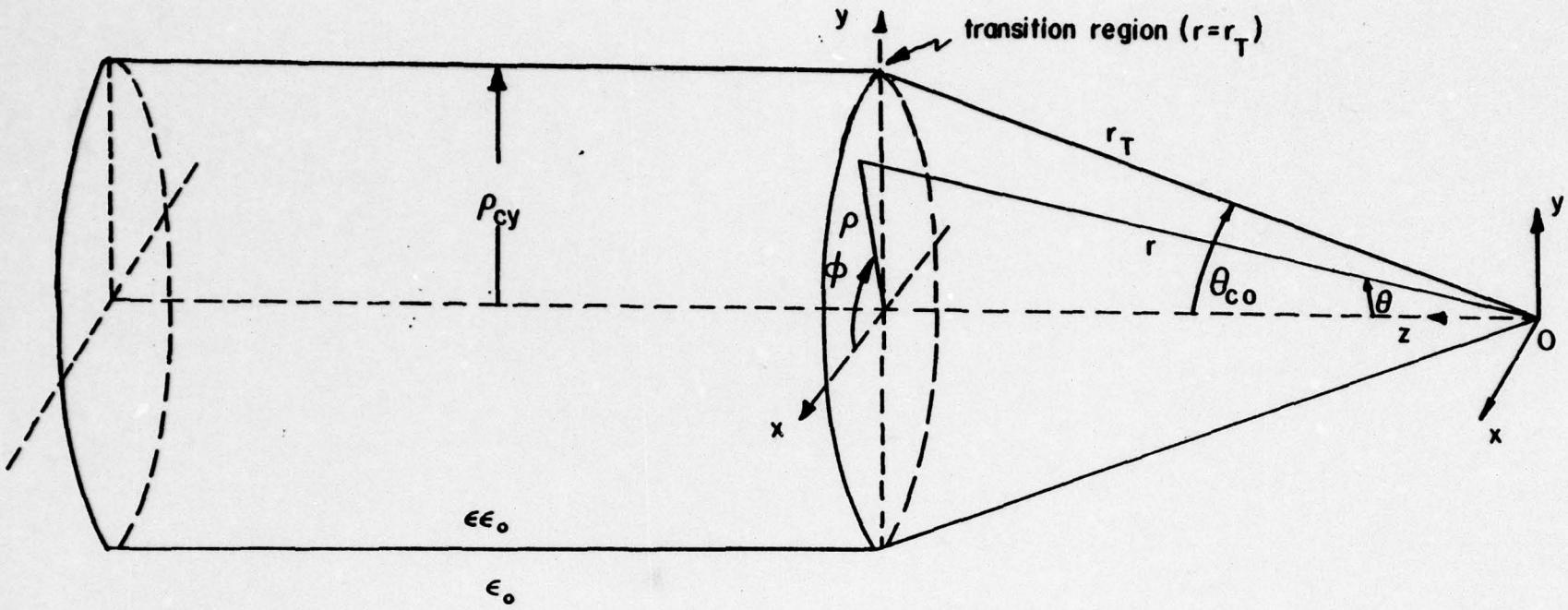

FIG. 1 Geometry and Coordinates of dielectric cylinder feeding dielectric cone.

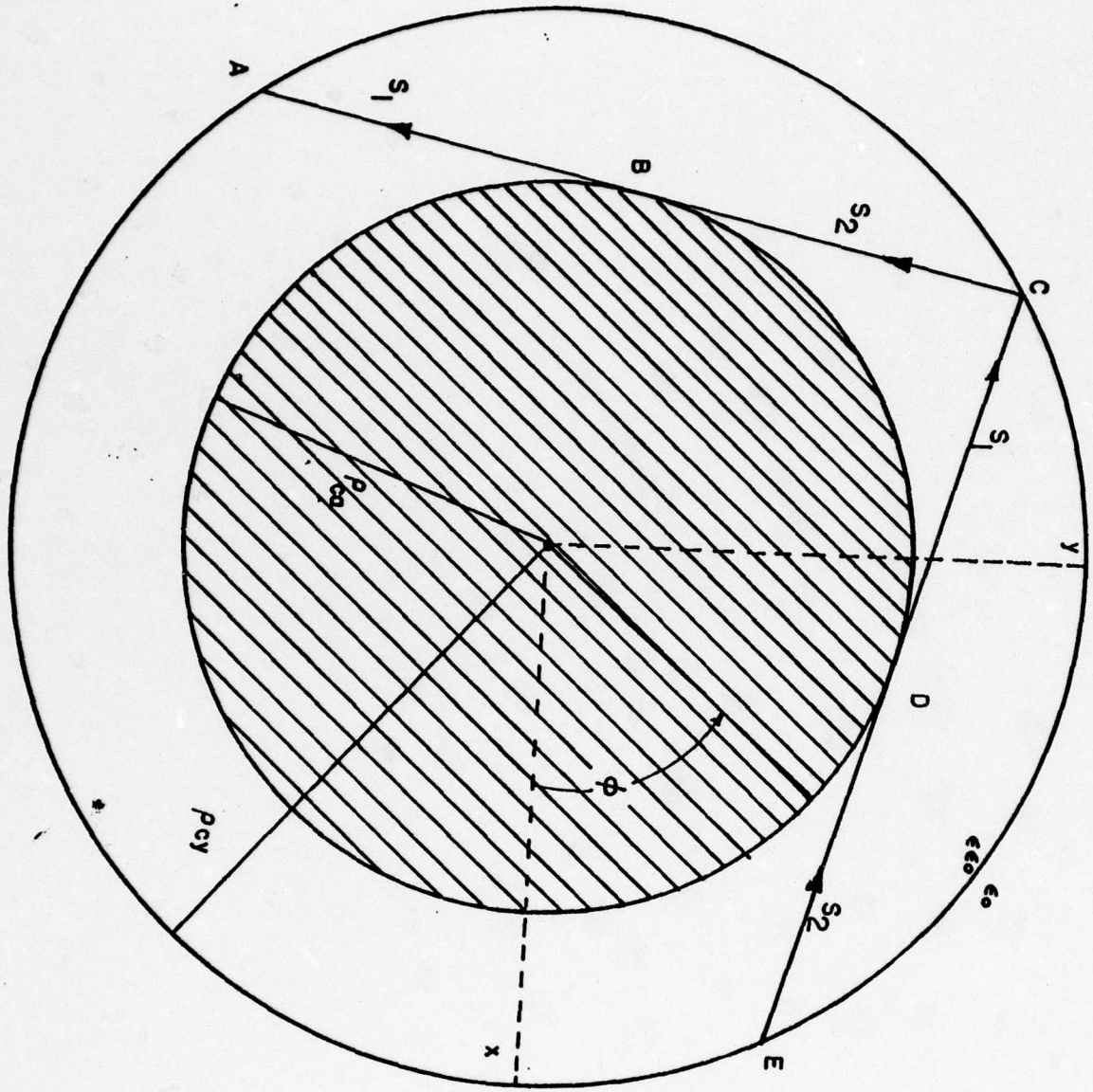

FIG. 2. Cross-sectional view of ray trajectories and caustic in the dielectric cylinder.

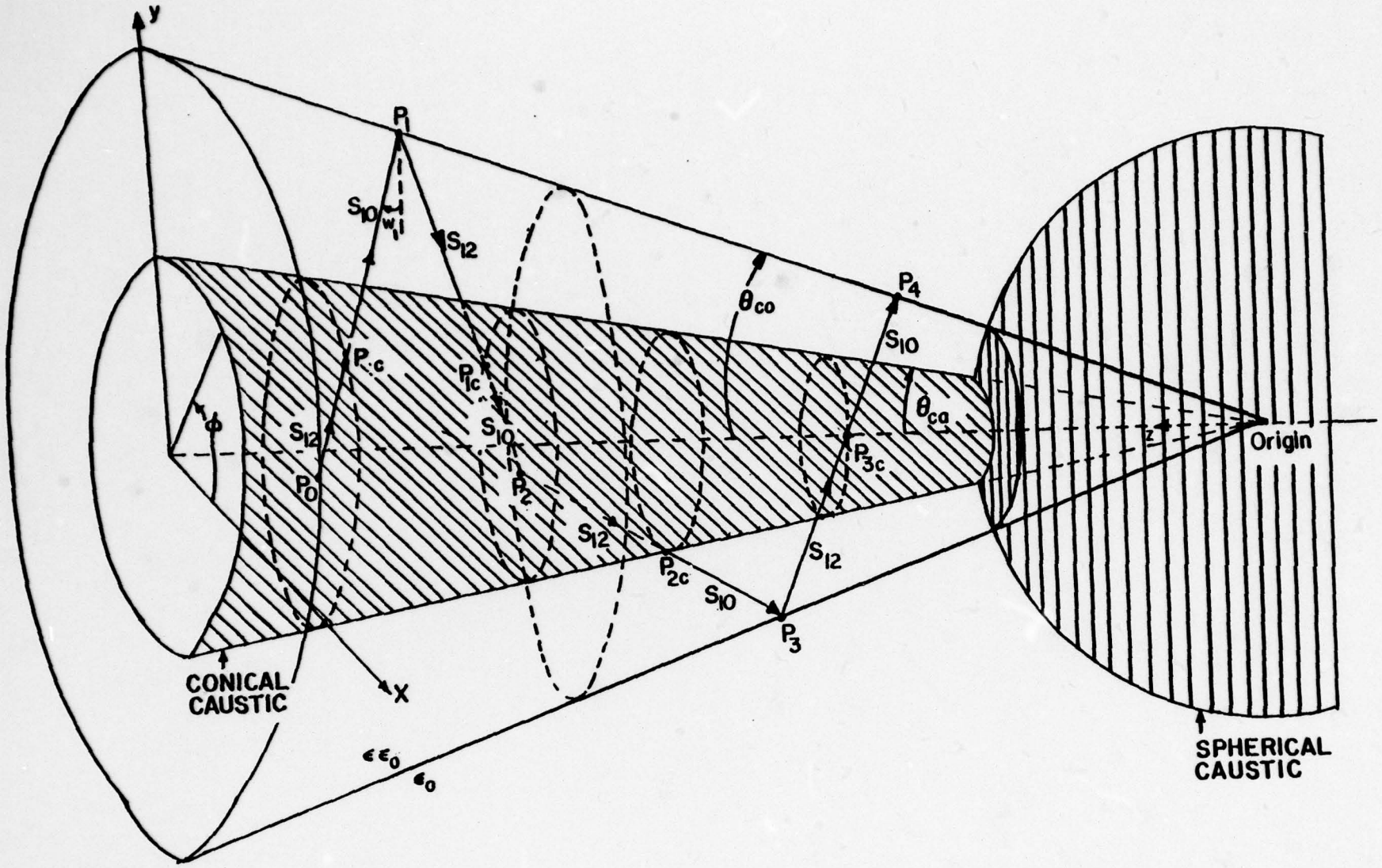

FIG. 3. Ray trajectories in the dielectric cone prior to reaching the spherical caustic.

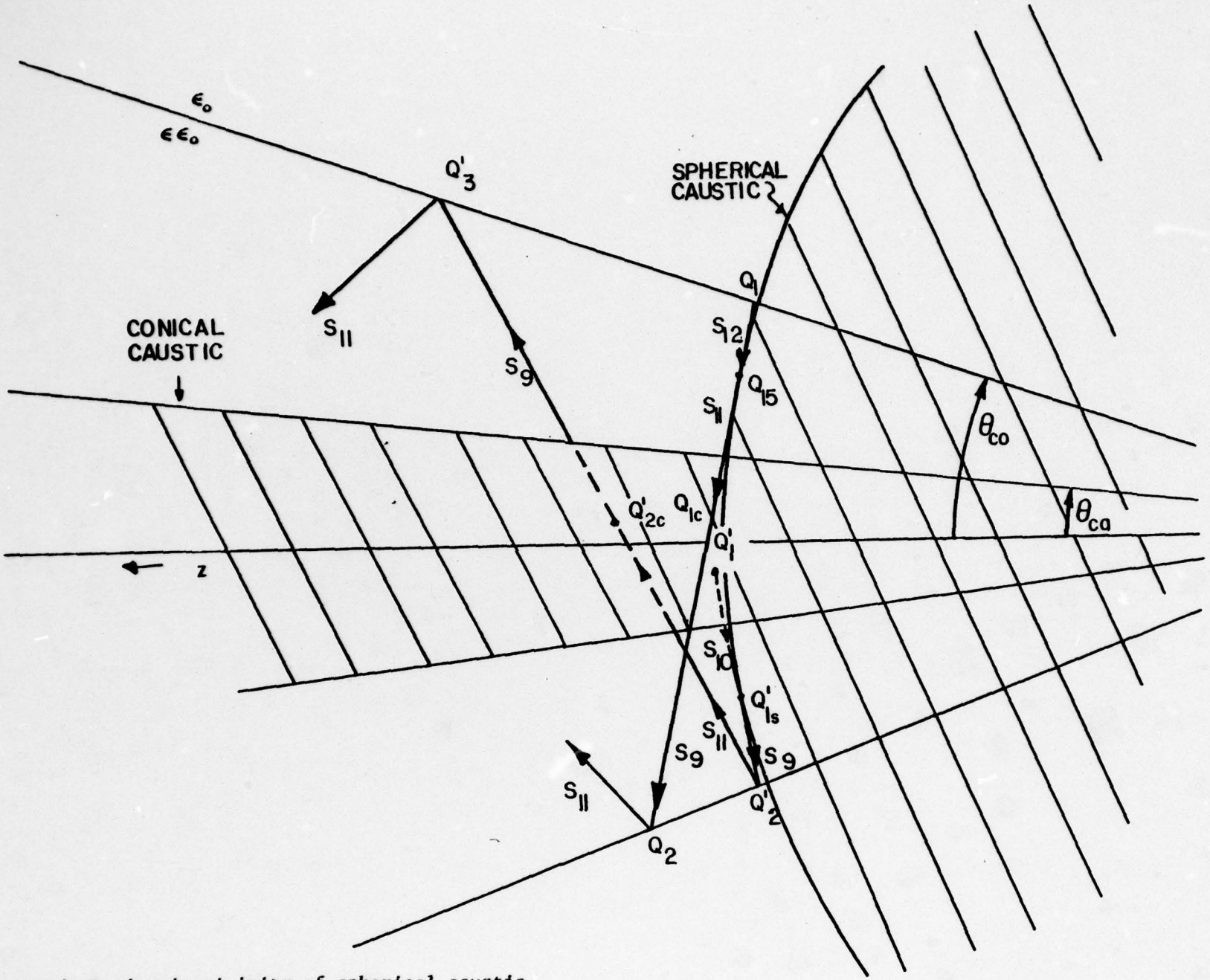

FIG. 4. Ray trajectories in vicinity of spherical caustic.

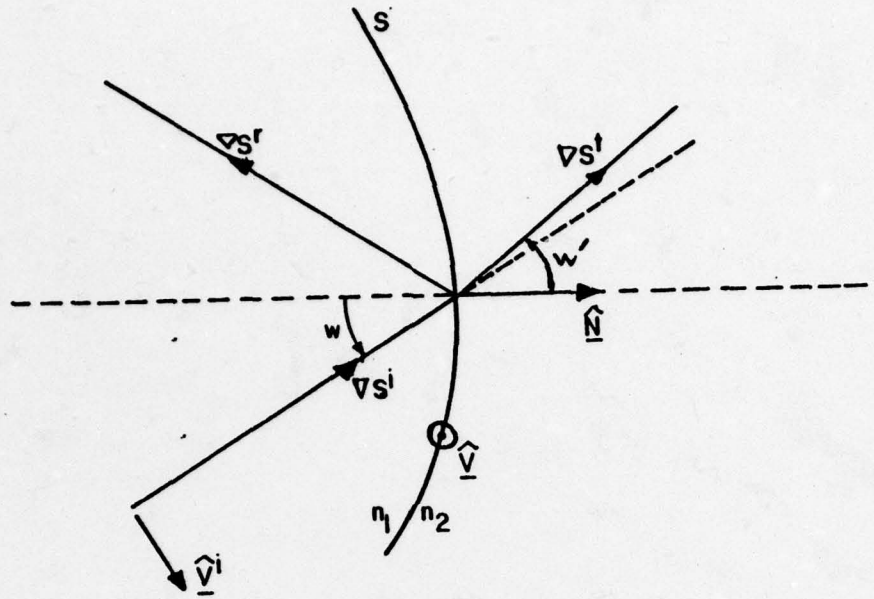

$$n_1 \sin w = n_2 \sin w'$$

FIG. 5. Reflection and transmission of rays at a curved interface between two dielectrics where $n_{1,2}$ are refractive indices

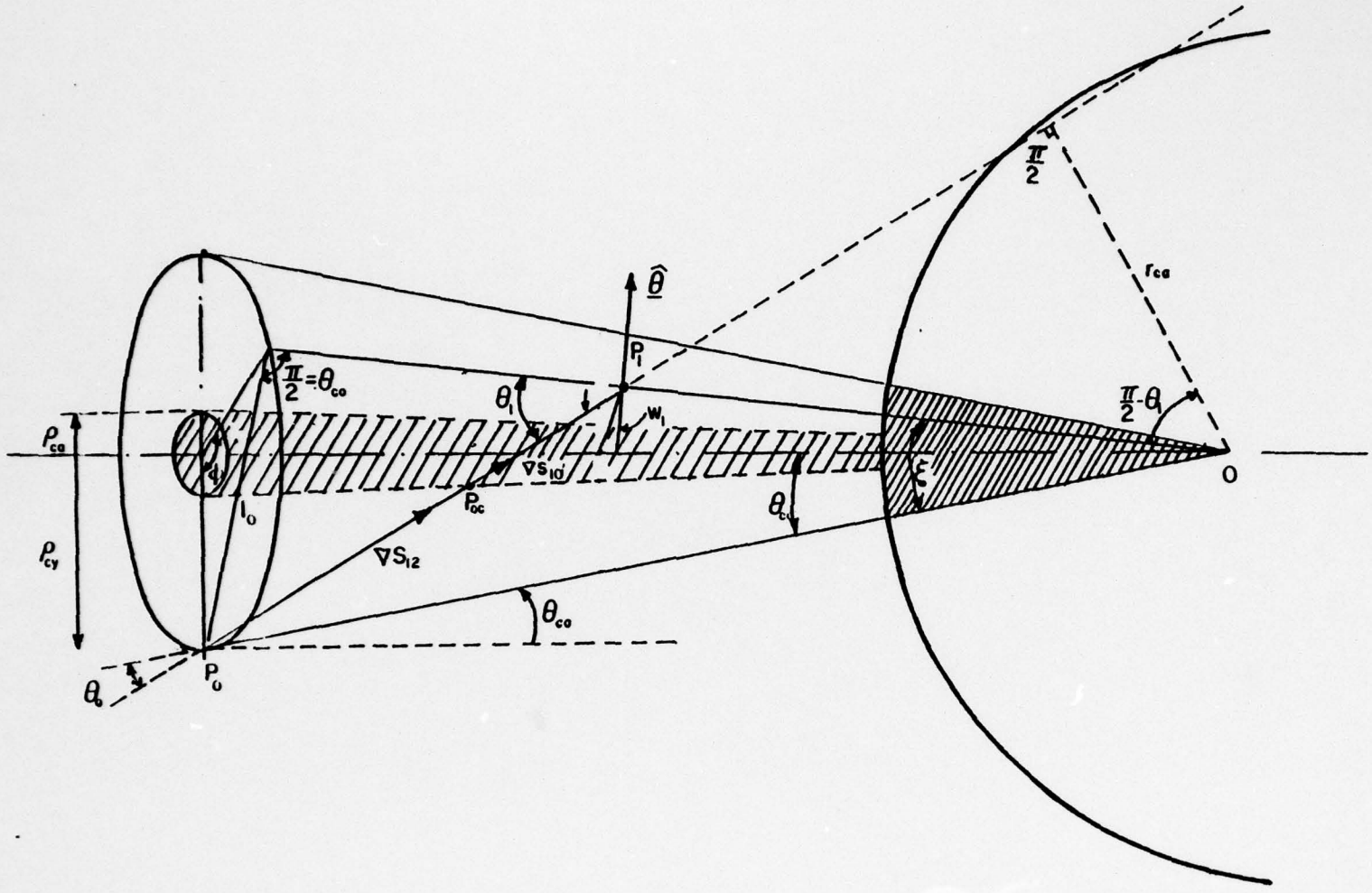

FIG. 6. Geometry for determining ray tracing in the dielectric cone.

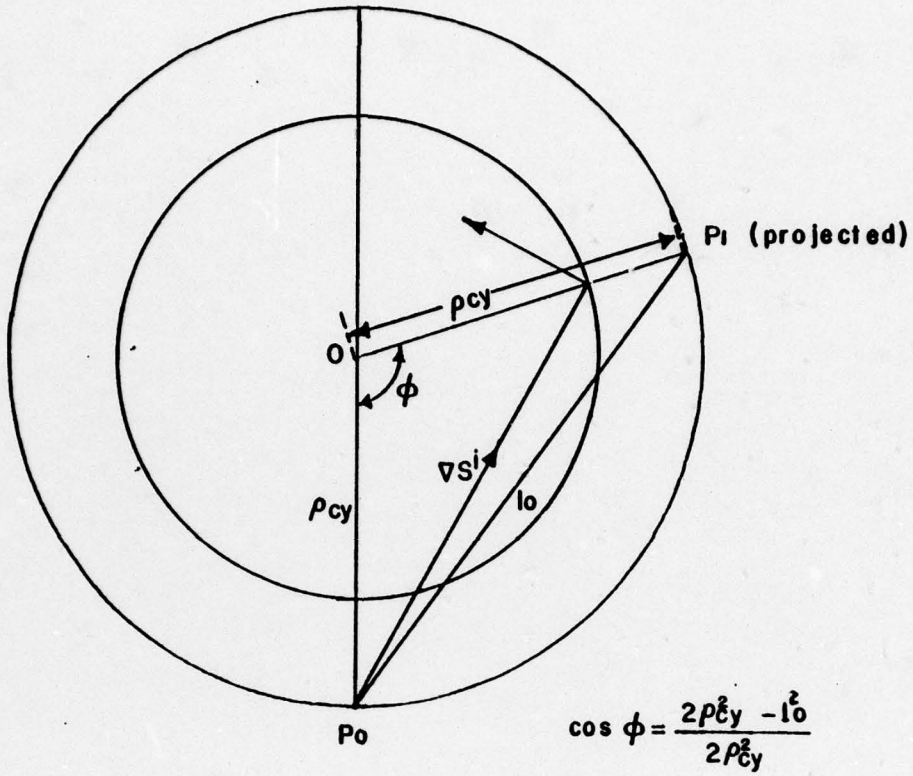

FIG. 7a. Projection on to the base of the cone (i.e., on to the termination of the cylinder) to determine the ϕ variation of a ray as it progresses toward the conical tip - a single reflection from the conical surface.

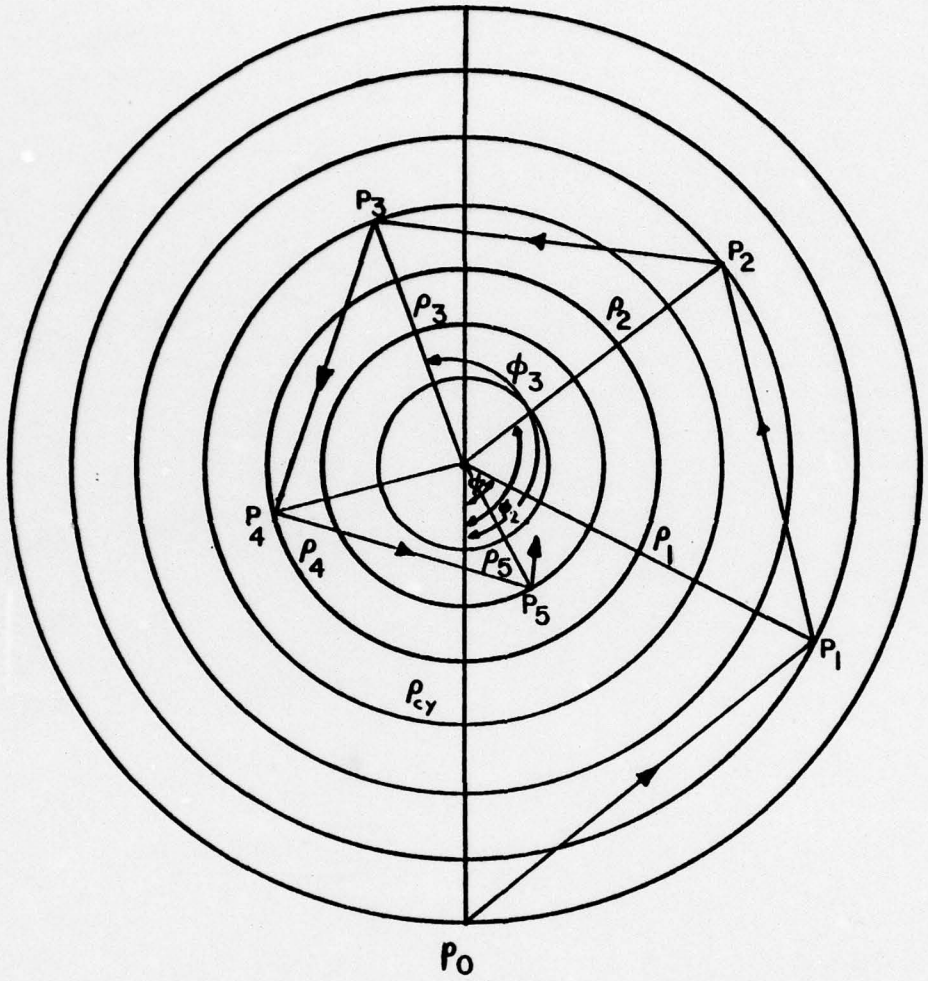

FIG. 7b. Projection on the base of the cone (i.e., on to the termination of the cylinder) to determine the ϕ variation of a ray as it progresses toward the conical tip - subsequent reflections from the conical surface.